OXFORD

Cerebral Cortex, 2023, 1–16
https://doi.org/10.1093/cercor/bhad408
Original Article

Intensive whole-brain 7T MRI case study of volitional control of brain activity in deep absorptive meditation states

Winson Fu Zun Yang[1,2], Avijit Chowdhury[1,2], Marta Bianciardi[2,3,4], Remko van Lutterveld[5,6], Terje Sparby[7,8,9], Matthew D. Sacchet[1,2,*]

[1]Meditation Research Program, Department of Psychiatry, Massachusetts General Hospital, Harvard Medical School, Boston, MA 02129, USA,
[2]Athinoula A. Martinos Center for Biomedical Imaging, Department of Radiology, Massachusetts General Hospital, Harvard Medical School, Boston, MA 02129, USA,
[3]Brainstem Imaging Laboratory, Department of Radiology, Athinoula A. Martinos Center for Biomedical Imaging, Massachusetts General Hospital and Harvard Medical School, Boston, MA 02129, USA,
[4]Division of Sleep Medicine, Harvard University, Boston, MA 02115, USA,
[5]Department of Psychiatry, UMC Utrecht Brain Center, University Medical Center Utrecht, CX Utrecht 3584, the Netherlands,
[6]Brain Research & Innovation Centre, Ministry of Defence, AA Utrecht 3509, the Netherlands,
[7]Steiner University College, Oslo 0260, Norway,
[8]Department of Psychology and Psychotherapy, Witten/Herdecke University, Witten 58448, Germany,
[9]Integrated Curriculum for Anthroposophic Psychology, Witten/Herdecke University, 58448 Witten, Germany

*Corresponding author: Meditation Research Program, Department of Psychiatry, Massachusetts General Hospital, Harvard Medical School, Boston, MA 02129, USA. Email: sacchetadmin@mgh.harvard.edu

Jhanas are profound states of mind achieved through advanced meditation, offering valuable insights into the nature of consciousness and tools to enhance well-being. Yet, its neurophenomenology remains limited due to methodological difficulties and the rarity of advanced meditation practitioners. We conducted a highly exploratory study to investigate the neurophenomenology of jhanas in an intensively sampled adept meditator case study (4 hr 7T fMRI collected in 27 sessions) who performed jhana meditation and rated specific aspects of experience immediately thereafter. Linear mixed models and correlations were used to examine relations among brain activity and jhana phenomenology. We identified distinctive patterns of brain activity in specific cortical, subcortical, brainstem, and cerebellar regions associated with jhana. Furthermore, we observed correlations between brain activity and phenomenological qualities of attention, jhanic qualities, and narrative processing, highlighting the distinct nature of jhanas compared to non-meditative states. Our study presents the most rigorous evidence yet that jhana practice deconstructs consciousness, offering unique insights into consciousness and significant implications for mental health and well-being.

Key words: advanced meditation; neurophenomenology; consciousness; 7T functional magnetic resonance imaging (fMRI); brainstem and thalamus.

Introduction

Meditation includes a variety of intentional awareness mental activities such as observing, focusing, and releasing the mind, with an underpinning of meta-awareness (Sparby and Sacchet 2021). Theravada Buddhism has been a major influence on contemporary meditation practices, offering extensive methodologies and descriptions of meditative practices and states. Its impact is evident in the growing popularity of mindfulness meditation among contemplative scientists and in society more broadly (Kang and Whittingham 2010; Samuel 2015). Consequently, there is growing appreciation for health-related benefits of meditation, and increasing interest in research to uncover its underlying mechanisms and limits (Van Dam et al. 2018).

The number of neuroscientific studies on meditation have surged in recent decades, leading to the emergence of contemplative neuroscience as a subfield, uncovering consistent effects in various brain regions and networks associated with meditation practices (Tang et al. 2015; Sezer et al. 2022). However, contemplative neuroscience has yet to rigorously investigate the advanced meditative states and stages that may be experienced through long-term and intensive practice. These states are part of meditative development (Galante et al. 2023) that culminate in meditative endpoints, such as cessation events that are associated with psychological clarity and openness (Laukkonen et al. 2023).

One advanced meditative state that is part of meditative development is jhana (*jhāna* in Pali, the liturgical language of Theravada Buddhism) (Buswell et al. 2014). Jhanas are advanced meditation states wherein the meditator develops immense concentration on the meditation object (Sayadaw 2008), leading to a temporary cessation of spontaneous mental content (Gunaratana 1988). These states are described as rich and profound sequences of increasingly deep states of unfettered calmness, clarity, ego-dissolution, and open consciousness (Gunaratana 1988; Hagerty et al. 2013; Yamashiro 2015; Dennison 2019; Sparby 2019). Jhanas offer unique insights into the nature of consciousness and are a significant focus in meditation practices. They can be characterized into two overarching types: the form jhanas

Received: August 7, 2023. **Revised:** October 9, 2023. **Accepted:** October 10, 2023

(*rūpa jhānas*) and the formless jhanas or realms (*arūpa jhānas* or *arūpa āyatanas*). The form jhanas are numbered by their progressive stages (J1 to J4), whereas the formless jhanas commonly are referred to by their primary phenomenological characteristics, but they can also be referred to as J5 to J8.

According to typical traditional accounts, the 1st jhana (J1), the first of the form jhanas, is characterized by the presence of five specific factors called the jhana factors: (1) directed attention; (2) sustained attention; (3) emotional joy, (4) mental ease, and (5) single-pointedness (Sayadaw 2008; Buswell et al. 2014). Meditators in J1 feel physical pleasure that permeates throughout the entire body (Brahm 2005). Physical pleasure and directed attention diminish during the subsequent experience of J2, characterized by the experience of intense emotional joy (zest) (Sayadaw 2008). Next when the emotional joy has subsided, what remains is characterized by the intense mental bliss and ease (J3). J4 is reached when mental bliss and ease of J3 subsides to reveal a deep experience of equanimity.

Consciousness and perception become increasingly highly refined in the next four jhanas (J5 to J8), the formless jhanas. Note that there is a gradual refinement of the jhana factors in J1-J4, while consciousness and perception becomes highly refined during J5-J8 (Sayadaw 2008). J5-J8 are very subtle and are increasingly difficult to describe. Here we provide brief definitions to contextualize their characteristics. J5 is termed as *infinite space*, in which the experience of boundless space fills the mind. J6 is termed *infinite consciousness* in which perception of boundless space disintegrates, and what remains is perception of single-pointed consciousness is maintained. Similarly, in J7 (termed *infinite nothingness*), the perception of infinite consciousness fades away to reveal very subtle perception of what might be termed infinite nothingness. Finally, in J8, termed *neither perception nor non-perception*, only an extremely subtle form of awareness remains.

As jhanas unfold, the level of attention on the meditation object becomes increasingly deeper as the meditator systematically relinquishes the predominant jhanic quality/qualities or characteristics associated with the given jhana. This process enables falling into the subsequent deeper jhana until the meditator reaches the eighth jhana, characterized by a state of minimal consciousness unaffected by external stimuli (Metzinger 2020).

With mastery, jhanas become relatively easily accessible and can easily recovered at will. They do not appear to be unique to just Buddhist meditation; other spiritual and religious practices such as the Carmelite tradition (Beauregard and Paquette 2006), Islamic Sufi meditation (Ernst 1998; Applebaum 2019), and Jewish contemplative traditions (Fisher 2022) have provided ample examples of similar states induced by or associated with sensory deprivation, immense attention, and self-generated bliss. Considering the well-documented history of jhanas described precisely, systematically, and rigorously by Theravada Buddhism, we focus on jhanas in this paper.

The study of jhanas is a new area within contemplative neuroscience. Although meditation research traditionally focuses on commonly studied topics such as perception, cognition, emotion, and clinical applications (Dimidjian and Segal 2015; Young et al. 2018; Keng et al. 2021), there is a growing interest in the characterizing phenomenological activities in meditation research (Sparby and Sacchet 2021). However, studying jhanas presents unique challenges due to difficulty in recruiting suitable expert meditators measuring these states objectively (Wright et al. 2023). Furthermore, the complex trajectories across jhanas require thoughtful experimental designs to assess these states (Galante et al. 2023). Nevertheless, the growing interest in advanced meditation and their potential benefits warrant continued investigation.

To our knowledge, there have been two prior neural studies of the jhanas: one electroencephalography (EEG) study (Dennison 2019), and the other a functional magnetic resonance imaging (fMRI) and EEG case study on an adept meditator (Hagerty et al. 2013). Of interest is the fMRI-EEG study where Hagerty et al. hypothesized, due to the phenomenology of these states, that jhanas should exhibit specific blood-oxygen-level-dependent (BOLD) signal changes in regions associated with sensory processing, language, spatial cognition, attention, reward processing, and motor control (Hagerty et al. 2013). They recruited a long-term Buddhist meditation practitioner with over 6000 hours of formal meditation practice to meditate and access J1 to J8. Transitions between jhanas were indicated using button presses. They used several general linear models to examine BOLD signal changes in predefined brain regions between conditions and included a comparison of jhanic states. Hagerty et al'.s results included reduced activation in visual and auditory processing areas and language, somatosensory, and posterior-parietal areas during jhanas compared to rest and access concentration (a state of stable concentration that occurs before entering J1). They also reported increased activation in the nucleus accumbens (NAc), orbitofrontal cortex (OFC), and anterior cingulate cortex (ACC), supporting their hypotheses that these regions were associated with specific phenomenology of the jhanas, including diminished external awareness, internal verbalization, sense of personal boundaries, and rhythmic movement. Their results support the conceptualization that the brain's internal reward system can be self-stimulated through volitional control of mental activity during advanced meditation.

While the study conducted by Hagerty et al. provides initial evidence for neural correlates of jhanas (Hagerty et al. 2013), neuroscientific understanding of these states remains limited for several reasons. Comparing brain activity during jhanas with a resting condition pose a challenge as experienced meditators may naturally dwell in meditative absorption during rest, thereby undermining the effectiveness of this control condition (Tang et al. 2012). Moreover, the absence of linking brain activity to phenomenological qualities of jhanas restricts extent to which conclusions can be made about relationships between brain activity and the phenomenology of jhanas. Finally, while Hagerty et al. selected regions of interest based on scientific hypotheses, these regions were ultimately limited in scope and did not encompass the full range of brain areas potentially relevant to jhanas. For example, in addition to other cortical and subcortical regions not evaluated by Hagerty et al., the brainstem and thalamus may be crucial during jhanas. These regions control perception of the external world (Tononi 2004, 2008; Sherman 2016, 2017; Solms 2018; Wolff and Vann 2019; Solms 2020; Wolff et al. 2021; Seo et al. 2022), and modulate attention and emotion (Solms 2018; George et al. 2019; Solms 2020; Cauzzo et al. 2022), which is highly altered during jhanas (Hagerty et al. 2013). To gain a more comprehensive understanding of their roles during jhanas, it is crucial to utilize higher magnetic field strengths like 7T fMRI to achieve greater sensitivity in capturing brain activity in these smaller regions (Colizoli et al. 2022).

Ultimately, conducting a comprehensive whole-brain neurophenomenological study of jhanas offers valuable insights into the relationship between brain activity and consciousness. It can also serve as a systematic tool to enhance general wellbeing and inform the development of more effective treatments for mental health conditions (Dimidjian and Segal 2015; Young et al. 2018;

Keng et al. 2021). Jhanas have inherent therapeutic qualities as they are self-generated blissful states achieved through volitional control of mental activity and the brain's reward system (Hagerty et al. 2013). The study of jhanas also provides unique possibilities to investigate the plasticity of the human brain and roles of different brain regions and networks involved in generating and maintaining altered states of consciousness (Carhart-Harris et al. 2014; Atasoy et al. 2017; Atasoy et al. 2018; Girn et al. 2022). Taken together, jhanas are multifaceted layers of human consciousness with broad implications for understanding and facilitating health and well-being.

In this context, the current study aimed to investigate the neuroscience of jhanas including linking the brain with phenomenology. Specifically, we sought to answer three key questions: (1) what are the patterns of brain activity that are associated with jhanas across the whole brain, including the cortex, subcortex, brainstem, and cerebellum? (2) How does brain activity during jhanas differ from activity associated with various cognitive processes? And (3) how does brain activity during jhanas relate to phenomenology? Due to a lack of prior studies and understanding of jhanas, we designed and conducted a comprehensive and exploratory neurophenomenological analysis encompassing whole-brain activity using high magnetic field strength of 7T. The novelty of using high-resolution 7T-fMRI lies in its detailed and precise examination and understanding of brain activity at the level of cortex, subcortex, brainstem, and cerebellum in the context of meditation, specifically jhana. We tested specific aims linking brain activity (regional homogeneity; ReHo) to jhanas and their phenomenology with stringent statistical thresholds. ReHo was chosen as an index of brain activity as it is a close derivative of its underlying neuronal processes (Zang et al. 2004). Moreover, we also highlighted the novelty of analyzing the brainstem and cerebellum and the general functioning of these regions in the context of meditation, specifically jhana meditation, at a high-resolution 7T-fMRI.

Materials and methods

Case study participant

Data were collected from one adept meditator, aged 51 years old at the time of the study. The participant is a long-term meditation teacher with over 25 years of jhana meditation experience at the time of data acquisition. Based on an estimated one hour of daily practice since the start of practice, and approximately one year of retreat at 14 hours per day, we estimate a total practice amount of 23,110 hours. Before the neuroimaging sessions, a clinician assessed the participant for neuropsychiatric diagnoses with the Mini-International Neuropsychiatric Interview (Sheehan et al. 1998) and found no neuropsychiatric diagnoses. The participant also showed no cognitive impairment as assessed by the Mini-Mental State Examination (Folstein et al. 1975). The Mass General Brigham IRB approved the study, and the participant provided informed consent.

The participant's meditation style during scanning was closer to the sutta-jhana than the Visuddhimagga-jhana as the participant reported using the breath, bodily feelings, and width of attention during the form jhanas, and formless objects (i.e. space, consciousness, nothingness, neither perception nor non-perception) as the jhana objects for entering the jhanas, rather than using the *nimitta* to enter them. The nimitta is the Pali term for the mental image of intense absorption on a meditation object, and is usually perceived as visual light (Brahm 2005; Kuan 2012). It is important to note here that different traditions and schools have different interpretation and techniques for teaching jhana meditation (Quli 2008; Snyder and Rasmussen 2009; Brasington 2015; Anālayo 2019). Contemporary jhana teachers and styles like the Pa Auk method or Mahasi Sayadaw method based their teachings and methods on the *Visuddhimagga* (Visuddhimagga jhanas), which uses the nimitta as an access point to jhanas and require very deep concentration. In contrast, sutta jhanas are "lighter" in concentration.

Experimental design

Jhana states

FMRI data were collected across five consecutive days. Depending on fatigue levels and comfort of the participant fMRI data collection during jhana for each day was approximately 45–90 minutes. We asked the participant to meditate using their standard *jhana* meditation sequence with eyes closed. A run started with the participant entering access concentration (AC), progressing through J1 to J8, and finishing with a post-J8 state that is sometimes termed *afterglow*, a post-jhanic state where happiness and bliss linger for a period of time (Buddhaghoisa 2010). For every transition from AC to J6, the participant pressed a button to indicate the start of the given state. The participant did not indicate transitions from J6 to J7 and from J7 to J8 because the practitioner indicated that this would have disrupted the continuation of jhana practice; that is, the natural traverse to the next state would have been interrupted. Therefore, following the button press indicating a transition to the J6, the next button press was only when the participant exited the J8 and entered the post-jhana afterglow. In total, we recorded 27 runs of jhana. In this study, we focused only on the jhana states (J1-J8). The average duration for a complete run for this set of analyses (J1 to J6–8) was 512.01 seconds (Table 1).

Control conditions

We developed two control conditions that would be used in comparison against meditation states. These control conditions were designed to engage the participant's mind with non-meditative cognitions. These conditions were carefully selected to be sufficiently engaging not to induce meditative states. We did not use a resting-state control condition because experienced meditators may enter meditative states (Tang et al. 2012). Indeed, in designing our paradigm consultation with our case study participant confirmed concerns regarding the possibility of entering meditation during resting-state. Yet, our case study participant reported having induced meditative states during both control conditions (see Differences in ReHo between specific jhanas and control conditions subsection in the statistical analysis section for further details).

The two different control conditions implemented in this study were: (1) memory control task: the participant was asked to reminisce the events of the past two weeks and narrate them in their mind, without moving their lips, for 8 minutes; (2) Counting control task: the participant was asked to count down, mentally without moving the lips, in decrements of 5 from 10,000 for 8 minutes. We collected two runs for each control condition, providing 16 minutes of data for each control task. The first run of the control tasks was collected before any meditation runs, while the second run was conducted on the fourth day of MRI data collection.

Phenomenology

We implemented a neurophenomenological approach in which systematic first-person descriptions of experience were used

Table 1. Dwell time in the jhana states.

Jhana	Mean (SD) time spent per run (in seconds)	Total time spent (in seconds)
1st Jhana (J1)	78.84 (35.41)	2128.60
2nd Jhana (J2)	91.94 (30.73)	2582.40
3rd Jhana (J3)	100.00 (71.15)	2699.90
4th Jhana (J4)	66.81 (24.60)	1803.80
5th Jhana (J5)	50.59 (13.76)	1365.90
6th–8th Jhana (J6–8)	123.84 (39.98)	3343.70

to provide precise elaboration of objective neuroimaging data (Lutz and Thompson 2003). Our participant systematically evaluated the mental and physiological processes relevant to the experience of jhanas as they manifested during jhana meditation. The participant first listed these phenomenological items to characterize his experience during meditation. The items were then reviewed to define appropriate rating scales and terminology. The participant rated these items immediately following a full jhana run (J1 to J8). The phenomenological items used in this study were: (1) *stability of attention*, defined as the calmness and tranquility from poor to excellent stability; (2) *width of attention*, ranging from narrow scope like a laser to very wide like a fish-eye lens; (3) *intensity of jhanas*, defined as how jhanic a particular jhana was; (4) *quality of J2* (joy) defined as energetic sensations in the body such as tingling, lightning-like or electric sensations, and one or more waves moving through the body; (5) *quality of J3* (mental ease), described as restful, calm, cool, subtle, and broad contentment); (6) *quality of J4* (equanimity) described as spacious, sublimely neutral, deep peace neutral equanimity; (7) *formlessness* of the formless jhana, described as not having any forms; (8) *sensations of early narrative thought stream*, described as the presence of narrative thought contents during the form jhanas; and (9) *sensations of late narrative thought stream*, described as the presence of narrative thought contents during the formless jhanas. Each item was rated from 1 to 10, with higher values indicating a stronger experience within the given item. Stability of attention, width of attention, and intensity of attention were rated for each jhana in each run (27 runs for each of 6 jhana states J1-J5 and J6–8), while qualities of jhanas (J2, J3, J4, and formlessness of J5 to J8) were rated for their corresponding jhanas, that is, one rating for each of the 27 runs. Finally, sensations of early and late narrative thought streams were separately rated for each of the 27 runs.

Neuroimaging acquisition

Neuroimaging scans were acquired using a 7T MR scanner (SIEMENS MAGNETOM Terra) using a 32-channel head coil. Functional imaging was performed using a single-shot two-dimensional echo planar imaging sequence with T2*-weighted BOLD-sensitive MRI, repetition time (TR) = 2.9 sec, echo time (TE) = 30 ms, flip angle (FA) = 75°, field of view (FOV) = [189 × 255], matrix = [172 × 232], GRAPPA factor = 3, voxel size = 1.1 × 1.1 × 1.1 mm3, 126 slices, interslice distance = 0 mm, bandwidth = 1540 Hz/px, echo spacing = 0.75 ms. Slice acquisitions were acquired for the whole brain, with interleaved slices, sagittal orientation, and anterior-to-posterior phase encoding. Opposite phase-encoded (i.e. posterior-to-anterior) slices with the same parameters were also acquired to perform distortion correction.

Whole-brain T1-weighted structural images were acquired as follows: TR = 2.53 sec, TE = 1.65 ms, inversion time = 1.1 sec, flip angle = 7°, 0.8 mm isotropic resolution, FOV = 240 × 240, GRAPPA factor = 2, bandwidth = 1200 Hz/Px. The participant's physiological (i.e. heart rate using pulse oximetry and respiration using breathing bellows) signal recordings were collected throughout the scanning session.

Neuroimaging preprocessing

Preprocessing steps were conducted at the level of MRI session and for all runs within that session. A session started each time the participant's position was localized in the scanner and lasted until the next localization was conducted. For each session, one reverse phase-encode EPI was collected for distortion correction across all runs for that session.

Preprocessing steps consisted of (1) de-spiking (3dDespike, AFNI); (2) RETROspective Image CORrection (RETROICOR) (Glover et al. 2000) using (ricor, AFNI) to regress out the effects of physiological (cardiac and respiratory) noise on data. We used a total of 10 regressors: four cardiac phase regressors (2nd order), four respiration phase regressors (2nd order), respiration volume per time convolved with the respiration response function (Birn et al. 2008), and heart rate convolved with the cardiac response function (Chang et al. 2009); (3) slice time correction (3dTshift, AFNI); (4) Distortion correction using opposite phase-encoded EPI (3dNwarpApply, AFNI); (5) motion correction (3dvolreg, AFNI) was done by registering each volume to a volume with the minimum outlier voxels within the brain-mask (i.e. a low-motion volume, determined based on the data); (6) Registering the anatomical dataset (T1) to a standard (MNI152_2009) template (@Sswarper, AFNI). This step includes multiple substeps: (6a) Bias-field correction of T1 image (3dUnifize, AFNI); (6b) Skull-strip T1 (3dSkullStrip, AFNI); (6c) Nonlinearly warp the T1 to the standard dataset (3dQwarp, AFNI). Registration from EPI to the standard template was done by concatenating all the transformation matrixes (distortion correction, motion correction, registration to anatomical, anatomical to standard) into one single registration. Additional preprocessing steps included: (7) Scrubbing: we scrubbed any volume with motion > 0.3 mm and had more than 5% outlier voxels (AFNI). Scrubbed volumes were removed from the data. Next, and finally, we conducted (8) regression: We regressed out the eroded CSF mask time course and motion parameters (3 translations, 3 rotations) per run and conducted band-pass filtering (0.01–0.1 Hz) by putting them in one single regression (3dDeconvolve, AFNI). Each fMRI run was then segmented into its different jhana states (27 runs for each jhana) or control conditions (2 runs for each condition comprised of 8 minutes for each run). Additionally, each control run was further broken down into one-minute segments to ensure comparability with the 2-minute segments of each jhana state. This resulted in a total of 16 segments for each control condition, providing a sufficient number for statistical comparisons with the jhana states.

Regional homogeneity analysis

Regional homogeneity (ReHo) is a measure of similarity in temporal activation pattern of a voxel and its nearby voxels (Zang et al. 2004). This measure of local functional connectivity within brain regions is a close derivative of underlying brain activity (Zang et al. 2004). A higher ReHo value indicates stronger synchronization of local brain regions, indicating greater functional connectivity in that region and thus an index of greater brain activity. ReHo uses Kendall's coefficient of concordance (KCC) as an Index of similarity of time series of a voxel and its nearest neighboring voxels. Therefore, computing KCC requires a cluster-size input to define the neighboring voxel space. In this study, we defined a cluster size of 27, that is: 1 voxel as the center and its 26 neighbors in a $3 \times 3 \times 3$ voxel cube space. In this study, we calculated the ReHo values for every segmented jhana run, standardized the ReHo values before smoothing the standardized ReHo maps using a 6 mm full-width half-maximum kernel. The standardized ReHo values were then parcellated using four different masks: (1) Schaefer-400 parcellation atlas for cortical areas (Schaefer et al. 2018); (2) 62 Tian subcortex atlas for subcortical regions (Tian et al. 2020); (3) 66 Bianciardi brainstem atlas (Bianciardi et al. 2016); and (4) Multi-Domain Task Battery (MDTB) functional cerebellar atlas (King et al. 2019). In total our parcellation/segmentation yielded 538 ReHo regions.

Statistical analysis

ReHo patterns across jhanas

Before running the linear mixed model analysis to assess changes in brain activity across jhanas, hierarchical time series clustering using dynamic time warping was used to extract the optimal number of polynomial trends based on their shape (Sakoe and Chiba 1978; Aghabozorgi et al. 2015). These polynomial trends would then be used to fit the polynomial order of the linear mixed models. This approach was conducted to understand trends in brain activity as the participant progresses across jhanas without overfitting the data (i.e. avoiding using the maximum number of tested polynomial trends). Dynamic time warping uses a dynamic (stretching and compressing) approach to minimize a predefined distance measure between time series to find an optimally aligned path between them (Sakoe and Chiba 1978; Aghabozorgi et al. 2015; Sardá-Espinosa 2019). The "optimal" alignment minimizes the sum of distances between the aligned elements. We extracted the shape of the time series using hierarchical time series clustering with dynamic time warping. The mean of the ReHo value for each ROI across jhanas was computed, yielding six ReHo values (one for each jhana period, J1 to J5 and J6–8) for each ROI for 538 ROIs. We then used the *R* package, *dtwclust*, to extract the number of k-shaped clusters, ranging from 2 to 10, for the jhanas (Sardá-Espinosa 2023). Various cluster validity indices were used to evaluate the optimum number of clusters, including Silhouette, Score Function, Calinski-Harabasz, Dunn, Davies-Bouldin, Modified Davies-Bouldin, and COP indices (Sardá-Espinosa 2019). These indices each return a number for optimum clusters in the data, and the number with the most count was used as the winning number of clusters. The shapes of the clusters were then used to create the polynomial order of the linear mixed model.

Linear mixed models were then used to analyze trends in brain activity across jhanas using the *lme4* (Bates et al. 2015) and *lmerTest* (Kuznetsova et al. 2017) packages. We set each run as a random intercept component, and jhanas as a random slope and fixed effect. The order of the polynomial slope was fit as a fixed effect; that is: if a cubic polynomial order was suggested by time series clustering, then the cubic term, along with its lower-order quadratic and linear terms, were included. In cases where the slope of the highest-order term was non-significant, that term was removed, and the model was rerun. This was repeated until the highest term became significant or only the linear term remained. This approach simplified and increased the interpretation of models. All analyses were corrected for multiple statistical comparisons across all 538 ROIs using false-discovery rate to reduce the number of false positives. Furthermore, models exhibiting singularity (indicating perfect multicollinearity among predictors) or non-convergence (resulting in unstable parameter estimates) were considered uninterpretable due to the challenges they pose in accurately determining the relationship between predictors and the outcome. Consequently, these models were not brought to the next stage of analysis even though their slopes may have been significant. All analyses were conducted in R (R Core Team 2022) loading on R Studio v2022.12.0.353.20 (Posit team. 2022).

Differences in ReHo between specific jhanas and control conditions

To characterize differences between jhanas and general cognition, we analyzed specific jhanas and conducted linear mixed models to compare against our two control conditions (memory and counting). As our participant reported experiencing jhanas during the first 8-minute runs of the control conditions, we also compared brain activity between jhanas and control conditions using only the last 8-minute runs (segments 9–16) of the control conditions as additional analyses.

We targeted analyses across jhanas, and then specifically on J1, J4, and J5 as they represent major milestones in the spectrum of jhanic-type consciousness. J1 is the entry of the jhanas, and J4 is the peak of the form jhanas. In contrast, J5 is the entry into the formless jhana. Each jhana was compared against brain activity assessed during the control conditions, thus yielding six sets of analyses (three for the memory control condition, and three for the counting control condition). In this set of analyses, segment number was set as a random intercept while the conditions were set as fixed effects, thus allowing for comparison of the difference in ReHo values between these conditions. All analyses were corrected within tests (538 ROIs) and across tests (six tests; one for each targeted jhana) using false-discovery rate to reduce the number of false positives. All additional analyses with the last eight-minute control runs (segments 9–16) were also corrected within tests (538 ROIs) and across the same six tests using false-discovery rate.

Relationship between jhanas and their phenomenological qualities

Pearson's correlation and multiple linear regression were used to assess neurophenomenological relations among brain activity during jhanas and phenomenological qualities as reported by the meditator. Specifically, we examined the (1) stability of attention; (2) width of attention; (3) intensity of jhanas across jhanas and runs; (4–7) quality of J2 (joy), J3 (mental ease), J4 (equanimity), and formless jhanas (J5 and J6–8; formlessness), and (8–9) sensations of narrative thought stream (early and late separately). This totaled in nine sets of correlational analyses. Pearson's correlation was used for sets 1 to 7 while linear regression was used for sets 8–9. This is because the former had phenomenology corresponding to each jhana and each run while sensations of narrative thought stream were rated for each run. As there were six ReHo values for six jhanas paired with only two sensation ratings in

each run, linear regression was the optimum choice to investigate the relationship between jhanas and sensations of narrative thought stream. Thus, two linear regressions were conducted with sensations of early and narrative processing as predicted outcome variables separately while ReHo values in J1-J4 (early) and J5 and J6–8 (late) as predictors. All analyses were corrected within tests (538 ROIs) and across tests (9 tests) using false-discovery rate to reduce the number of false positives.

Physiological signals control analysis

We conducted several linear mixed models to ensure that physiological signals were constant across jhanas. Apart from regressing out physiological noise in our fMRI data, this set of tests was conducted to ensure that changes in brain activity across jhanas were due to the meditation, not physiological signal change, such as cardiac or respiratory rate. We set each run as a random intercept component, jhanas as a random slope and fixed effect, and modeled the averaged cardiac and respiratory signals separately over each run as outcome variables. Additionally, we corrected for two multiple tests using false-discovery rate. We also compared physiological signals between specific jhanas (J1, J4, J5) and the counting control condition, yielding six tests in total. In this set of analyses, segment number was set as a random intercept while the conditions were set as fixed effects, thus allowing for comparison of the difference in physiological signals values between these conditions. All analyses were corrected within tests (cardiac and respiratory) and across tests (3 tests; one for each targeted jhana) using false-discovery rate to reduce the number of false positives.

Data and code availability

Data may be requested and subjected to the Institutional Review Board's approval. All code used in this study may be made available by request from the corresponding authors.

Results

Hierarchical time-series clustering

Time-series cluster validity indices found that the optimum number of clusters was two (Fig. 1). The first cluster is a quadratic shape, while the second cluster is a cubic shape. Therefore, quadratic and cubic slopes were added to their corresponding linear mixed models as appropriate. A positive quadratic slope indicates a U-shaped curve whereby ReHo values decrease and then increase. In contrast, with a negative quadratic slope, ReHo values first increase and then decrease across jhanas. Cubic slopes are wave-like instead: positive cubic slopes increase until their peak, decrease until their trough, and increase again. The pattern is opposite for the negative cubic slopes, whereby ReHo values decrease in ReHo values until reaching a trough, and then rise until reaching a crest, followed by a decrease.

ReHo patterns across jhanas

Linear mixed models revealed three significant unique brain activity trends in various brain regions as the meditator traversed the jhanas. To simplify the interpretation of the data, we group and report the results using cortical, subcortical, brainstem, and cerebellum schemes. A pattern observed was that regions associated with positive quadratic and cubic trends were mostly regions with negative linear trends, and vice versa for negative quadratic and cubic trends. See Fig. 2 for additional details, Supplementary Table S1 to S4 for detailed nomenclature of all the regions, and Supplementary Table S5 for a list of significant regions.

Cerebral cortex

Positive linear ReHo trends were found in bilateral temporal, visual, posterior, parietal, somatomotor, orbitofrontal (OFC), insulae, and ventral medial prefrontal (vmPFC) regions, and within the right cingulum. In contrast, negative linear ReHo trends were identified in bilateral dorsolateral prefrontal (dlPFC) regions, temporal poles, and left medial prefrontal (mPFC) regions. Quadratic trends were mostly negative, that is, we observed inverted U-shaped curves that peaked at J4 and J5 before descending. Negative cubic trends are mostly negative, and are shown by decreasing ReHo values until reaching a trough, and then rising until reaching a crest, followed by a decrease.

Subcortex

Positive linear trends were identified the bilateral thalamic nuclei, left anterior globus pallidus (aGP), left lateral amygdala, left head l1 of the hippocampus (left HIP head l1), and right nucleus accumbens shell (NAc shell). Negative linear trends were found in the bilateral thalamic nuclei, left caudate, and right putamen.

Brainstem

Positive linear trends were identified in the periaqueductal gray (PAG) and left superior colliculus; and negative linear trends in the right locus coeruleus and vestibular nuclei complex (Ve).

Cerebellum

Positive linear trends were found in cerebellar functional regions 8, 9, and 10, associated with word comprehension, verbal fluency, and autobiographical recall, respectively.

Quadratic and cubic trends were also found in the brainstem, with positive quadratic trends in the bilateral laterodorsal tegmental nucleus (central gray of the rhomboencephalon; LDTg_CGPn), Ve, left dorsal mesencephalic reticular formation (mRtd), oral and caudal parts of the pontine reticular nucleus (PnO_PnC), subcoeruleus, and right locus coeruleus (LC), and negative quadratic trend in the left substantia nigra part 2 (SN2) and right medial part of the lateral inferior medullary reticular formation (iMRtl).

In contrast, positive brainstem cubic trends were found with the left mRTd, right LC, LDTg_CGPn, and Ve.

Differences in ReHo between specific jhanas and control conditions

Comprehensive results, summary tables of significant regions are shown in Supplementary Table S6. Results are visualized in Fig. 3 and comprehensive statistical maps organized by brain slices are included in Supplementary Fig. 2. Here, we only provide a summary of the results.

Jhana vs memory control condition

J1 was associated with higher ReHo values in the bilateral prefrontal, temporal, somatomotor cortices, several nuclei of the hippocampus, putamen, and thalamus, several nuclei of the right reticular formation (Rt), and cerebellum functional region 10; and negatively associated with ReHo values in the bilateral somatomotor, temporal, visual cortices, right temporo-occipito-parietal cortex, precuneus, left NAc core, right hippocampus, left lateral inferior olivary nucleus, parabrachial nucleus, raphe nuclei, right RN, Rt, viscero-sensory-motor nuclei complex, and cerebellum, among other regions. J4 and J5 were associated with similar positive and negative ReHo values in the cortex, subcortex, and cerebellum.

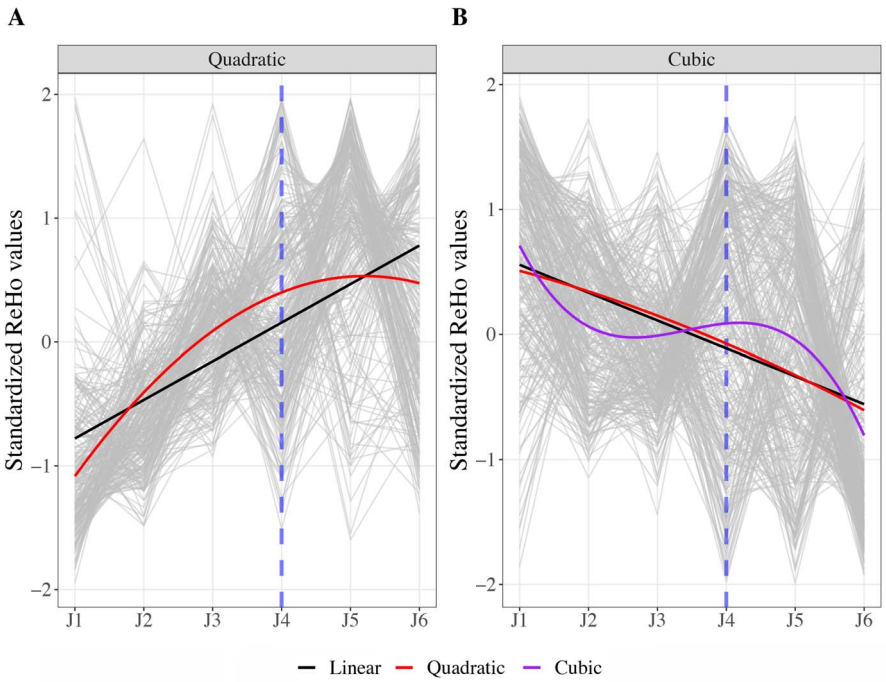

Fig. 1. Clusters of ReHo trends from hierarchical time series clustering. Standardized and normalized ReHo values for each ROI across jhanas are represented as gray lines. The dotted line represents the fourth and final jhana of the form jhanas, separating form and formless jhanas. Two clusters of time series were found using hierarchical time series clustering with dynamic time warping, time series with a quadratic trend and cubic trend.

However, in the brainstem, J4 was associated with positive ReHo values in the left SN and right Rt, and negative ReHo values in the left pedunculotegmental nucleus (PTg), right inferior colliculus, and parabrachial pigmented nucleus complex of the ventral tegmental area (VTA_PBP). J5 was associated with positive ReHo values in the left SN, VTA_PBP, right Rt, and superior colliculus, while negatively associated with ReHo values in the left lateral parabrachial nucleus and right inferior colliculus.

Jhana vs counting control condition

J1 was associated with higher ReHo values in the bilateral temporal poles, right OFC, PFC, somatomotor cortex, right dorso-anterior putamen, and cerebellum functional region 10; and negative ReHo values in the bilateral somatomotor cortices, left medial cortex, precuneus, right posterior, parietal cortices, bilateral hippocampus, left AMY, NAc core, putamen, right thalamus, raphe nuclei, PAG, bilateral Rt, left LC, right VTA_PBP, and the cerebellum. J4 and J5 were associated with similar positive and negative ReHo values in the cortex, subcortex, and cerebellum.

In the brainstem, J4 was associated with negative ReHo values in the left PAG, bilateral Rt, left LC, medial parabrachial nucleus, PnO_PnC, right RN, and VTA_PBP. J5 was associated with positive ReHo values in the left SN, while negatively associated with ReHo values in the bilateral Rt, left PnO_PnC, subcoeruleus, right alpha part of the parvicellular reticular nucleus (PCRtA), RN, and Ve.

Differences in ReHo between specific jhanas and control conditions (segments 9–16 only)

Comprehensive statistical maps organized by brain slices are included in Supplementary Fig. 3. Here, we only provide a summary of the results.

Jhana vs memory control condition

Compared to the memory control condition, J1 was associated with higher ReHo values in bilateral inferior temporal, left anterior temporal, right dorsal anterior, somatomotor, insula, left head of the hippocampus, right putamen, and cerebellar functional region 10; and lower ReHo values in the bilateral middle temporal, posterior, visual, and cerebellar functional region 7.

J4 was associated with higher ReHo values in left visual, inferior temporal, anterior temporal, and posterior regions, right putamen, left SN2, and cerebellar functional region 10; lower ReHo values in the bilateral PFC, medial prefrontal (MPFC), middle temporal areas, left dorsoanterior medial thalamus, and cerebellar functional region 10.

Finally, J5 was associated with higher ReHo values in bilateral visual, somatomotor, inferior temporal regions, left anterior temporal, insula, posterior, SN2, and cerebellar functional region 10; lower ReHo values in the bilateral PFC, MPFC, right middle temporal regions, and cerebellar functional region 10.

Jhana vs control control condition

Compared to the counting control condition, J1 was associated with higher ReHo values in bilateral visual cortex, OFC, posterior cortex, temporal poles, and right aGP; and lower ReHo values in the bilateral precuneus, PFC, hippocampus, somatomotor areas, thalamic nuclei, RN, SN, left temporal cortex, iMRTl, LDTg_CGPn, LPB, mRta, PnO_PnC, Ve, right amygdala, IC, and VTA_PBP. J4 and J5 was associated with similar positive and negative ReHo values in the cortex, subcortex, and brainstem. In the cerebellum, J4 was associated with negative ReHo values in the cerebellar functional region 7. J4 was also associated with positive ReHo values in the right GP and putamen.

Relations among jhanas and phenomenology

Pearson's correlation revealed unique patterns of relations among various brain activity values during jhana and their phenomenological qualities. Comprehensive result tables are included in Supplementary Table S6. Comprehensive statistical

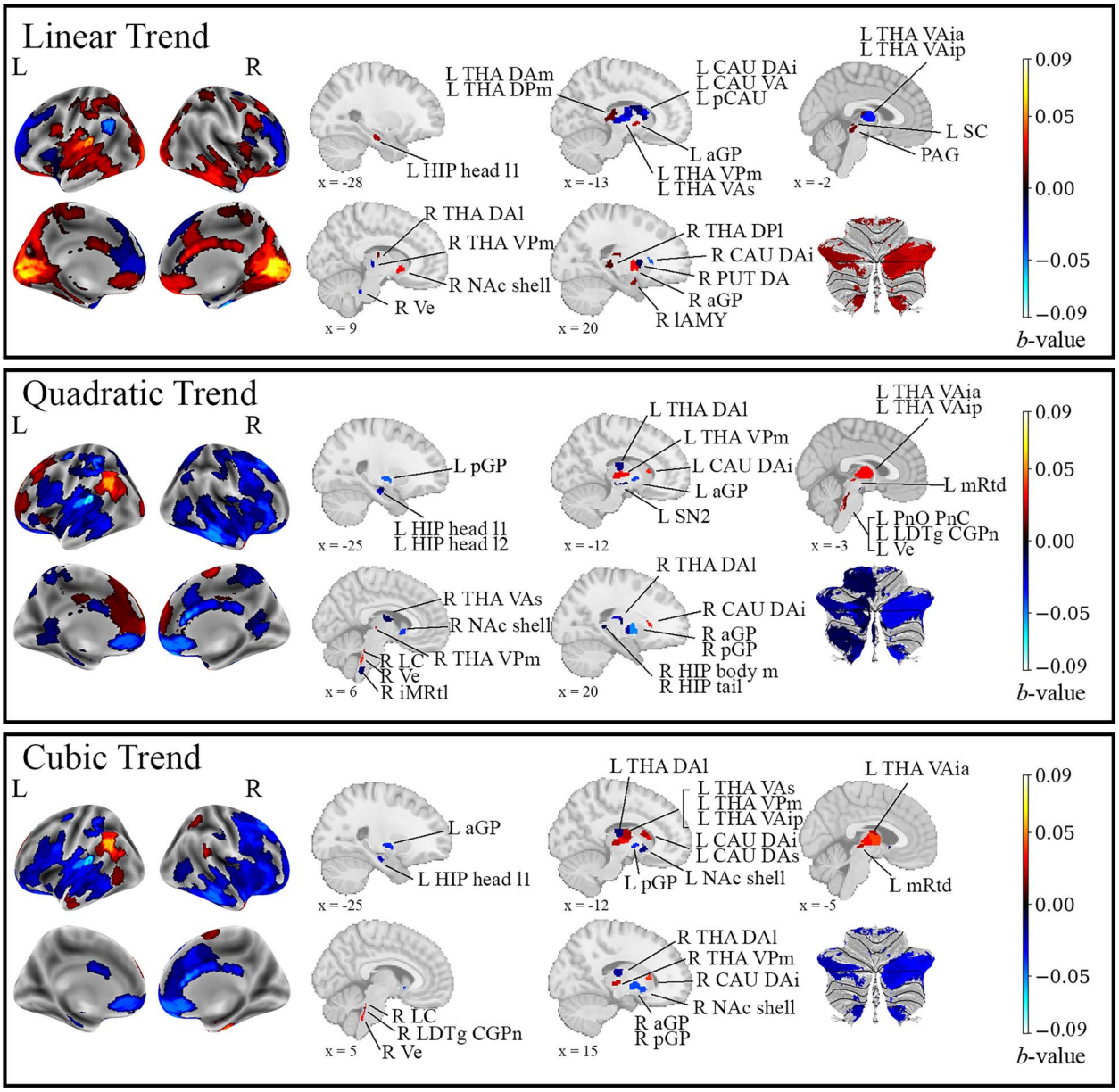

Fig. 2. Whole-brain ReHo trends. Whole-brain ReHo trends across jhanas were separated into clusters with either linear, quadratic, or cubic trends. Positive linear trends indicate increasing ReHo values across jhanas (J1 to J6–8), while negative linear trends indicate decreasing ReHo values across jhanas. A positive quadratic trend indicates a U-shaped curve whereby ReHo values decrease and then increase. In contrast, with a negative quadratic trend, ReHo values first increase and then decrease across jhanas. Cubic trends are wave-like instead: Positive cubic trends increase until their peak, decrease until their trough, and increase again. The pattern is opposite for the negative cubic trend, whereby ReHo values decrease in ReHo values until reaching a trough, and then rise until reaching a crest, followed by a decrease. Additional visualizations by brain slices are included in Fig. S1. AMY = amygdala, CAU = caudate, GP = globus pallidus, HIP = hippocampus, LC = locus coeruleus, LDTg CGPn = Laterodorsal tegmental nucleus—Central gray of the rhomboencephalon, MRt = medullary reticular formation, NAc = nucleus accumbens, PAG = periaqueductal gray, PnO PnC = oral and caudal parts of the pontine reticular nucleus, PUT = putamen, RN = red nucleus, SC = superior colliculus, SN = substantia nigra, SubC = subcoeruleus, THA = thalamus, Ve = vestibular nuclei complex, L = left, R = right, a/a = anterior, D/d = dorsal, i = inferior, l = lateral, m = medial, P/p = posterior, s = superior, V/v = ventral. Detailed nomenclature for all regions is provided in Table S1 to S4.

maps organized by brain slices are included in Supplementary Figs. 4–6c.

Stability of attention, width of attention, and intensity of jhanas

higher ReHo values in the bilateral posterior, parietal, and visual cortices, and lower ReHo values in the bilateral dlPFC, mPFC, OFC, and insulae were associated with higher intensity of all three ratings separately.

We also reported the subcortex, brainstem, and cerebellum associations for stability of attention, width of attention, and intensity of jhanas. First, higher stability of attention was associated with higher ReHo values in the bilateral thalamic nuclei, left aGP, and right Rt, and negative ReHo values in the left caudate, hippocampus, NAc core, putamen, bilateral PTg, and cerebellum. Second, higher width of attention was associated with higher ReHo values in the thalamus and cerebellum, and negative ReHo values in the left caudate, putamen, LDTg_CGPn, PCRtA,

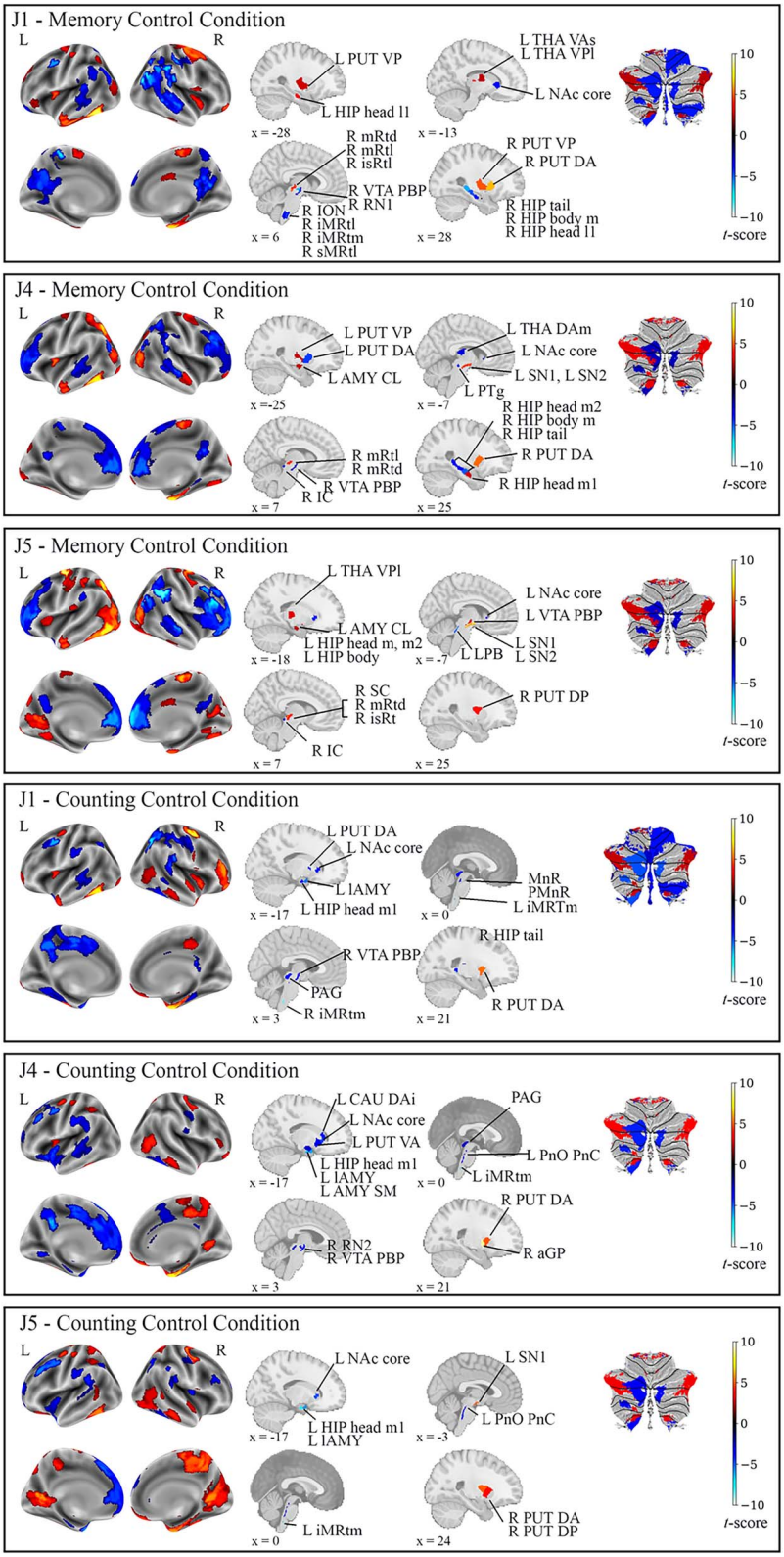

Fig. 3. ReHo differences between jhanas and control conditions. This figure visualizes differences in brain activity (ReHo values) between the first jhana (J1), fourth jhana (J4), and fifth jhana (J5), and the memory and counting control conditions. The memory control condition requires the participant to reminisce the events of the past two weeks and narrate them in their mind, without moving their lips, for 8 minutes. In contrast, the counting control task requires the participant to count down, mentally without moving the lips, in decrements of 5 from 10,000 for 8 minutes. Additional visualizations by brain slices are included in Fig. S2. Detailed nomenclature for all regions is provided in Table S1 to S4.

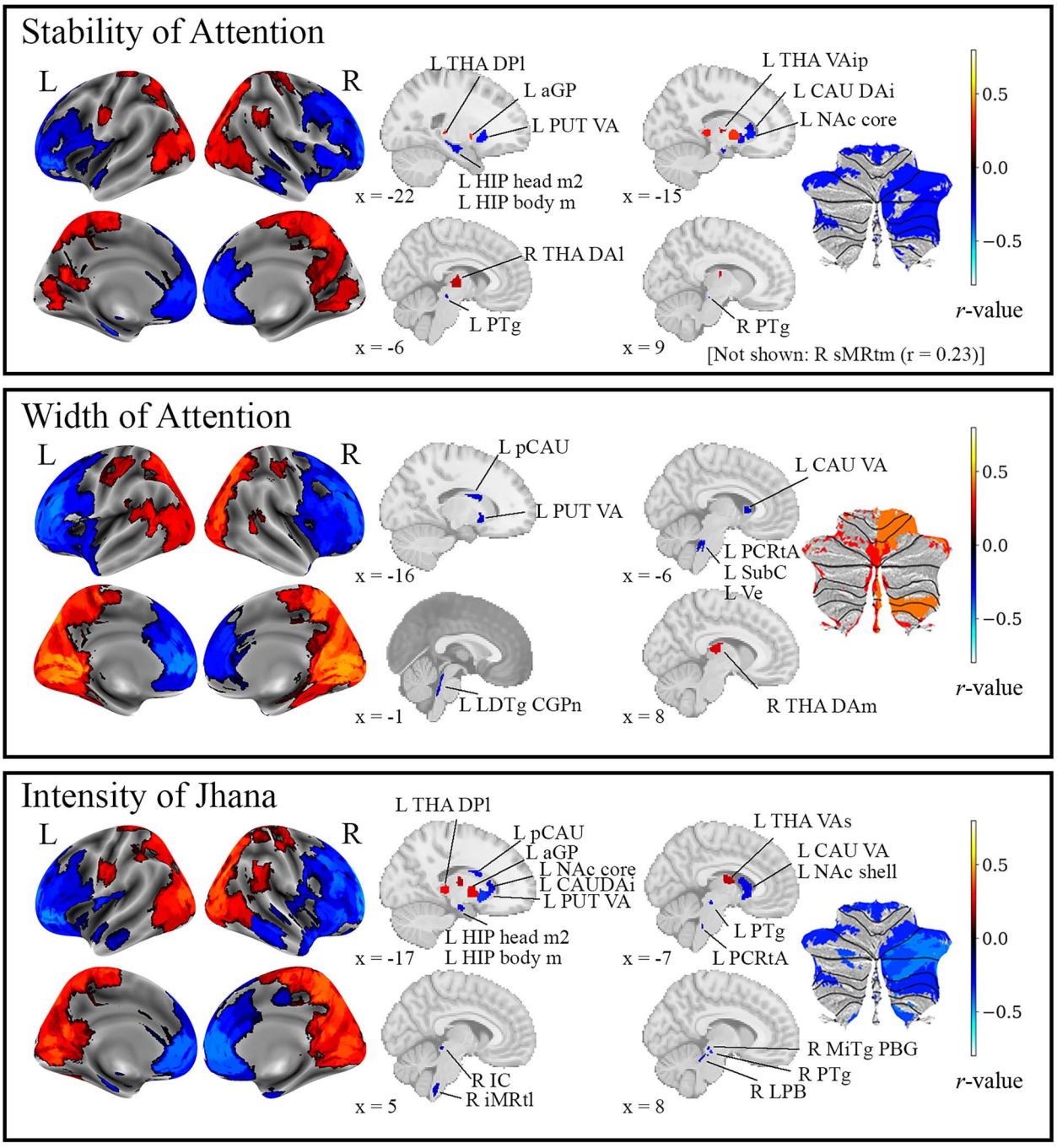

Fig. 4. Correlation between ReHo values and qualities of attention and intensity of jhanas. For every run and every jhana, the participant reported the stability, width of attention, and intensity of jhana. Pearson's correlation was used to compute the correlation between whole-brain ReHo values and the qualities of attention, and intensity of jhanas. All correlational tests were corrected with false-discovery rate to reduce the number of type I errors across all correlational tests (538 regions × 9 phenomenology items). We observed clear distinctions in correlations between self-reported attentional qualities and ReHo values in the anterior and posterior cortical brain regions. Additional visualizations by brain slices are included in. Figure S4. Detailed nomenclature for all regions is provided in Table S1 to S4.

subcoeruleus, and Ve. Finally, higher intensity of jhanas was associated with higher ReHo values in the left aGP and thalamic nuclei, and lower ReHo values in the several nuclei of the caudate, hippocampus, NAc, putamen, bilateral PTg, left PCRtA, right inferior colliculus, Rt, lateral parabrachial nucleus, and parabigeminal nucleus of the microcellular tegmental nucleus (MiTg_PBG). Results for the relationship between ReHo and the attentional qualities of stability of attention, width of attention, and intensity of jhanas are visualized in Fig. 4.

Jhana quality

Higher quality of J2 (joy) was associated with higher brain activity in right somatomotor areas and lower values in the right temporal regions. Higher quality of J3 (mental ease) was associated with higher ReHo values in the visual and posterior cortices, and lower ReHo values in the insulae, OFC, cingulum, temporal cortex, as well as the left hippocampus body, and cerebellum. Higher quality of J4 (equanimity) was associated with higher ReHo values in the bilateral visual and right parietal areas, and lower ReHo values

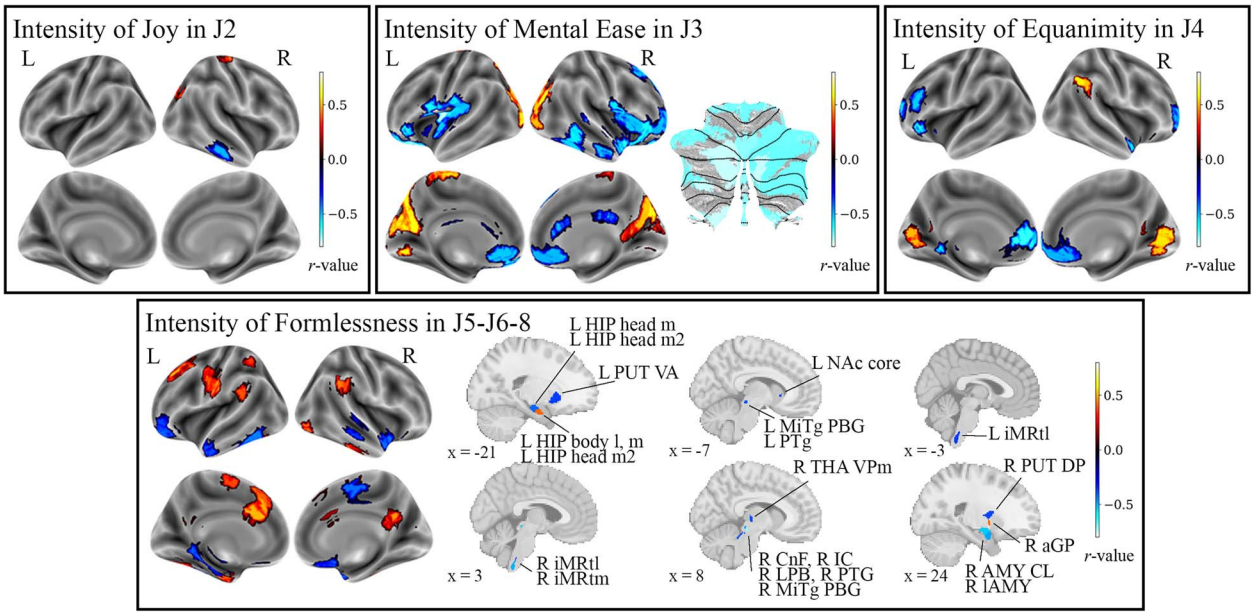

Fig. 5. Correlation between specific characteristics of each jhana and ReHo values, specifically (A) intensity of joy and J2; (B) intensity of mental ease and J3; (C) intensity of equanimity and J4; and (D) intensity of formlessness in the formless Jhanas. Intensity of formlessness ratings from J6 to J8 were averaged to match the neuroimaging data in J6–8. We also grouped formlessness as a single construct rather than separating it into J5 and J6–8 to reduce the number of correlational tests. Additional visualizations by brain slices are included in Fig. S5. Detailed nomenclature for all regions is provided in Table S1 to S4.

in the bilateral dlPFC, lPFC, and left PTg. Finally, higher quality of formlessness was associated with higher ReHo values in the bilateral parietal cortices, left somatomotor cortex, lPFC, bilateral aGP, left head of the left hippocampus, and thalamus, and lower ReHo values in the bilateral temporal cortices, right supplementary motor area, bilateral putamen, left nuclei of the hippocampus, NAc, right amygdala, putamen, thalamus, bilateral Rt, MiTg_PBG, right cuneiform nucleus, inferior colliculus, lateral parabrachial nucleus, and PTg. The correlational results for the relationship between ReHo and specific jhanic qualities are included in Fig. 5.

Sensations of narrative thought stream

Higher sensations of early narrative processing were associated with higher J2 ReHo values in the left lPFC, J3 ReHo values in the right temporal and somatomotor cortices, and J4 ReHo values in the left PFC and visual cortex; and negative J2 ReHo values in the right parietal, posterior, somatomotor cortices, J3 ReHo values in the bilateral somatomotor cortices, left lPFC, J4 ReHo values in the right parietal, temporal, and somatomotor cortices. In contrast, sensations of late narrative processing were associated with positive J6–8 ReHo values in the left hippocampus, NAc, right thalamus, and negative J6–8 ReHo values in the left posterior cortex. Visualizations of the regression weights for the relationship between ReHo and sensations of narrative thought stream are shown in Fig. 6.

Physiological signals confound across jhanas

Linear mixed model revealed no significant linear change in either cardiac ($t = 0.42$, $P > 0.05$) or respiratory ($t = 0.49$, $P > 0.05$) signals across jhanas. Comparing jhanas (J1, J4, and J5) and the counting control condition, there were no significant differences in cardiac signals for J1 ($t = -0.50$, $P > 0.05$), J4 ($t = -1.26$, $P > 0.05$), and J5 ($t = 0.37$, $P > 0.05$) compared to the counting control condition. For respiratory signals, there was a significant difference in respiratory signals for J1 ($t = 3.64$, $P = 0.01$), but not for J4 ($t = -0.931$, $P > 0.05$) and J5 ($t = 2.19$, $P > 0.05$).

Discussion

Using an intensive case study design, we conducted an exploratory while extensive neurophenomenological analysis of brain activity during jhana meditation. Our study is comprehensive in that we analyzed brain activity at the whole-brain level, including the rarely studied brainstem and cerebellum at high spatial resolution using ultrahigh field-strength fMRI data and stringent statistical thresholding levels. This is the second MRI study of jhana to date, and the most rigorous. We report several key findings: (1) patterns of local brain activity are unique across brain regions and jhanas; (2) brain activity during jhanas is unique from ordinary states of consciousness; and (3) phenomenological qualities of jhanas are represented by specific brain activations. Our data supported the phenomenology of advanced meditative practices using modern neuroscientific and neurophenomenological approach. These results provide considerable value in advancing the study of consciousness and wider applications of jhana practices in a psychological context.

One notable finding of this study is that jhana states and their phenomenology are associated with specific patterns of local brain activity. Jhanas are progressive and systematic states of consciousness unfolding with increasing depth of attention, decreasing levels of narrative processing, and the emergence of positive affect and rewards (Gunaratana 1988). According to the many-to-(n)one model of the predictive mind, confining attention to one object during meditation reduces prediction formation, prediction error signaling, and the temporal depth of processing (i.e. the narrative self) (Laukkonen and Slagter 2021). Consequently, there may be a reduced tendency to maintain other predictions, such as those related to the narrative self. In support of these characteristics, we revealed unique ReHo brain activation patterns in several brain regions associated with jhana phenomenology during systematic traversing of increasingly deeper layers of absorptive meditation.

We first discuss the attentional qualities of jhanas. We found positive linear trends in visual, affective areas (NAc, OFC, lateral

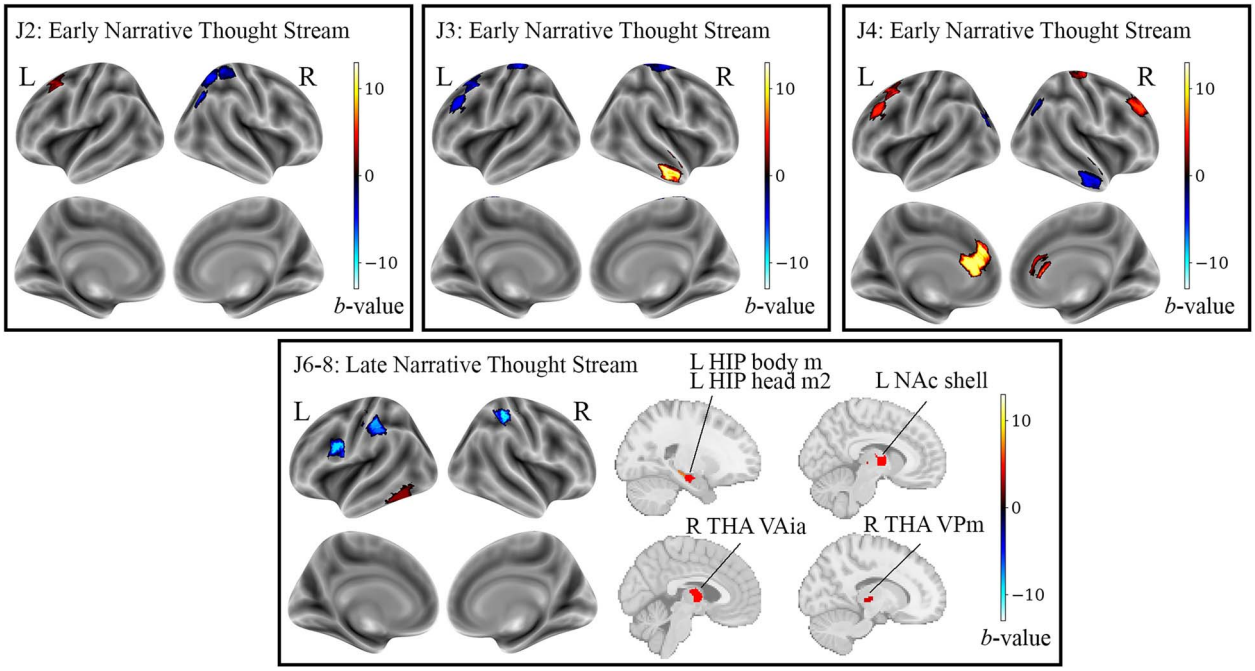

Fig. 6. Correlation between ReHo values and sensations of narrative thought stream. We reported regression weights between ReHo values and early (J1-J4), and late (J5-J6–8) sensations of narrative thought stream. As there were two ratings per run, one for early sensations, and another for late sensations, we conducted two linear regression models to examine the associations between linear combinations of jhanas within their respective groups and narrative processing. The figure shows significant associations between sensations of narrative thought stream and J2, J3, J4, and J6–8. There were no significant associations in J1 and J5. In J6, we observed additional significant associations between ReHo values in the subcortical regions and sensations of late narrative processing that were not found in the other jhanas. Additional visualizations by brain slices are included in Fig. S6. Detailed nomenclature for all regions is provided in Table S1 to S4.

amygdala), dorsal thalamic nuclei, PAG, superior colliculus, and several functional regions of the cerebellum. Although it seems contradictory to expect activations in the visual areas because sensations become inhibited during jhanas (Hagerty et al. 2013), jhanas are often accompanied and preceded by the experience of what is sometimes termed *nimitta* in the Pali language. The nimitta is a mental image of intense absorption on a meditation object, and is usually perceived as visual light (Brahm 2005; Kuan 2012). We found that ReHo of the visual cortex increases with the depths of jhanas, supported by greater stability and width of attention, indicating a potential neural marker for stronger meditative absorption. While the evidence strongly supports the theory that attentional capacities and potentially the nimitta are linked to activity in visual brain regions, cautious need to be taken in interpreting this result as there may be other causes for visual activation other than greater attention during jhanas (Lindahl et al. 2014). Moreover, the participant reported using the breath, bodily feelings, and width of attention during the form jhanas, and formless objects (i.e. space, consciousness, nothingness, neither perception nor non-perception) as the jhana objects for entering the jhanas, rather than using the nimitta to enter them. This differ from other methods of reaching the jhanas, such as using the nimitta (Quli 2008; Snyder and Rasmussen 2009; Brasington 2015; Anālayo 2019). Therefore, caution is needed with interpreting the activity of the visual cortex with respect to attentional qualities of the jhanas and the nimitta. Future studies on jhana meditation would need to test this hypothesis in greater depth.

Additionally, we found a posterior–anterior cortical differentiation in the relationship between brain activation and attentional qualities (stability and width of attention) and intensity of jhanas. Higher attentional qualities and experiential intensity of jhanas were associated with increased brain activation in posterior cortical regions (e.g. parietal, visual cortices), and lower ReHo values in the anterior cortical regions (e.g. dlPFC, mPFC, OFC). Within the non-cortical regions, we also reported positive correlations in various thalamic nuclei, globus pallidus, cerebellar functional regions associated with right-hand presses and saccades, and negative correlations in several caudate nuclei, ventral anterior putamen, reticular formation nuclei, and several functional regions of the cerebellum.

Our comparisons with non-meditative states of cognition also indicated that jhanas were associated with an anterior–posterior brain reorganization, with negative ReHo values traveling from the medial posterior (e.g. visual cortex, precuneus) to anterior (e.g. ACC and mPFC) cortical brain regions. Additionally, we observed changes in various brain regions such as increased activation and deactivation in various nuclei of the thalamus, putamen, caudate, hippocampus, reticular formation, other brainstem nuclei, and cerebellum when comparing different jhana milestones with the control conditions.

This posterior–anterior differentiation in the cortex reflects the cortical hierarchy of the brain along the posterior–anterior axis in the cortex, from early sensory to higher-order transmodal cortices (Mahjoory et al. 2020). Here we report that increased meditative absorption during jhanas is related to reductions in top-down processing and increases in bottom-up brain processing, reflecting a deactivation of the narrative (Fox et al. 2016; Brandmeyer and Delorme 2018), cognitive control (Lieberman et al. 2019), goal-oriented processing, and goal predictions (Ribas-Fernandes et al. 2019). Our neurophenomenological analyses revealed positive associations between narrative processing and brain activity in frontal and temporal regions of the default mode network, as well as hippocampal and thalamic nuclei at J6, suggesting the role

of the thalamus in gating the construction of a self (Buckner and DiNicola 2019).

Jhana meditation deconstructs the unified conscious space into layers of raw experiences of consciousness (Tononi 2004, 2008), contrary to the brainstem-thalamic pathway's role as an informational "bottleneck" for emotion processing (Venkatraman et al. 2017) and the reticular formation's function in maintaining a unified conscious self (Faraguna et al. 2019). Jhanas are considered preparatory stages for the cessation of mental events, with the brainstem and thalamus playing a vital role (Laukkonen et al. 2023). We utilized a high-resolution 7T fMRI scan sequence designed for deep brain and brainstem data collection at small resolution for the brainstem. The involvement of the brainstem cannot be explained by physiological noise as they have been regressed out and showed no effects with jhana. Our findings underscore the importance of the brainstem and thalamus in constructing conscious experience and highlights the value of jhana meditation as a model for investigating consciousness. Together these effects generate an overarching shift in functional brain reorganization on the deconstruction of mental models of the self (Andrews-Hanna et al. 2010).

Next, we discuss the changes in affect, arousal, and reward processing during jhanas. We showed positive linear trends in affective regions that may indicate increased arousal and reward processing during jhana meditation. The NAc and OFC are highly activated during the experience of pleasure (Sabatinelli et al. 2007), while the basolateral amygdala is understood to encode motivationally salient, reward-specific representations such as pleasure to guide behavior (Wassum and Izquierdo 2015). In contrast, the PAG is thought to underlie the regulation of arousal and autonomic signals from other key affective regions (Quadt et al. 2022). Pleasant sensations and high arousal generated during jhanas could thus be related to activation within these regions. As the experiential layers of jhanas unfold volitionally, we report increases in the activation of brain regions associated with pleasure and reward.

In contrast, our neurophenomenological analyses revealed different regions linked to affect, arousal, and reward processing. We showed positive associations between brain activity in the right somatomotor and visual areas, among other regions, and joy in J2, and mental ease in J3, while negative associations in the right temporal cortex for joy and mental ease, and additionally bilateral insulae, OFC, right cingulum, left body of the hippocampus, and several cerebellar functional regions associated with saccades, divided attention, narrative processing, and word comprehension for mental ease. Equanimity (J4) showed positive associations with brain activations in bilateral visual cortices and right parietal cortex, while negative associations in bilateral OFC, left lateral PFC, and PTg. The evidence suggest that as the meditator progresses from J2 (joy) to J4 (equanimity), the value of rewards (joy and mental ease) diminishes, leading to the deactivation of the cerebellum (Adamaszek et al. 2016), OFC, and its projection to the insula, cingulum, PFC, and temporal cortex (Rolls et al. 2020).

Our findings of nonlinear quadratic and cubic brain activation trends indicate that these trends are not caused by distractions during meditation as suggested by Hagerty et al., but instead indicate genuine non-linear relationship between brain activity and jhanas (Galante et al. 2023). Specifically, we observed decreasing trends in somatomotor, prefrontal, temporal, parietal, and posterior cortical regions, head of the hippocampus, NAc, globus pallidus, red nucleus, substantia nigra, the cerebellum, and increasing in the dorsal caudate, ventral thalamic nuclei, and various reticular formation nuclei in the brainstem. While positive linear trends were found in the attention and affective regions, these brain regions exhibited negative quadratic and cubic trends.

Our results differ from Hagerty et al'.s in several ways. Hagerty et al. provided initial evidence on brain activity during jhana meditation but lacked precision as they did not include phenomenological analysis (Hagerty et al. 2013). While they found decreased activation in the visual, auditory and language cortical brain regions, we found the opposite. The phenomenology of jhanas can vary from individual to individual due to its primary and secondary features (Sparby 2019). Moreover the jhana meditator Hagerty et al. recruited was trained in the Sri Lankan tradition of jhanas by Khema (Khema 2001), which differs from our participant. Our neurophenomenological analysis found a positive correlation between the stability and width of attention, as well as the intensity of jhanas, and activity in visual brain regions, supporting the theory that attentional capacities and nimitta may be linked to visual activity. Next, Hagerty et al. studied only specific cortical and subcortical regions while we were very comprehensive in our analysis by including the cortex, subcortex, brainstem, and cerebellum at high spatial 7T resolution. Additionally, we used stringent statistical thresholding to reduce the number of false positives in our results.

This study has considerable strengths including analyzing neurophenomenology at the whole-brain level (cortex, subcortex, brainstem, cerebellum) at high spatial resolution using ultrahigh field-strength fMRI data, but also several notable limitations. First, using button presses to indicate transitions between jhanas may be imperfect. The intensity of jhanic absorption increases with deeper jhana states, making it challenging for meditators to signal transitions to deeper levels of jhanas (Gunaratana 1988; Brahm 2005). In fact, the participant could not indicate transitions to J7 and J8 as it would disrupt their meditation practice. While results related to J6 should be interpreted in caution given that data related to J6 to J8 were undifferentiated, these results still provide insight into neural patterns associated with deep experience of formlessness.

Second, the neural patterns and phenomenology found in this case study cannot be generalized to all jhana practices due to variations in meditation tradition, philosophy, and training methods (Sparby 2019). However, our case study is carefully designed to systematically quantify jhana states in neuroscientific methodology that are challenging to conduct in group studies. While our results may be specific to the individual, there is compelling evidence to suggest that these neurophenomenological closely correspond with the descriptions of jhanas found in ancient contemplative texts. Hence, future studies should empirically investigate the descriptions of jhanas found in ancient contemplative texts using modern neurophenomenological methods.

Finally, we attempted to create control conditions that were sufficiently engaging to not induce meditative states, the participant still reported that they performed some degree of insight meditation and reflection during the memory control condition. We can thus only make limited inferences regarding how jhanas compare with other non-meditative states of consciousness. Furthermore, it remains unclear how jhana compares to other altered states of consciousness, such as comatose states or those induced by psychedelic/entheogenic substances. Future studies should examine and compare jhana states with other altered states of consciousness, including other advanced meditative states.

Conclusion

In conclusion, jhanas are characterized by multifaceted gradations of consciousness that can be studied through

neurophenomenological approaches. Here we identified a rich array of unique brain activity patterns elicited by jhana meditation. We found that brain states associated with jhanas are distinct from those of non-meditative states of consciousness, and that these brain states are linked to phenomenological qualities. This study provides a strong foundation for further investigation of advanced meditative states and ultimately, a scientific understanding that facilitates the scaling of these states to more individuals.

CRediT taxonomy

Winson Fu Zun Yang (Formal analysis, Software, Visualization, Writing—original draft, Writing—review & editing), Avijit Chowdhury (Investigation, Software, Writing—review & editing), Marta Bianciardi (Investigation, Methodology, Software, Writing—review & editing), Remko van Lutterveld (Writing—review & editing), Terje Sparby (Investigation, Methodology, Writing—review & editing), Matthew D. Sacchet (Conceptualization, Funding acquisition, Investigation, Methodology, Project administration, Resources, Supervision, Writing—original draft, Writing—review & editing).

Supplementary material

Supplementary material is available at *Cerebral Cortex* online.

Funding

Dr Sacchet and the Meditation Research Program are supported by the National Institute of Mental Health (Project Number R01-MH125850), Dimension Giving Fund, Ad Astra Chandaria Foundation, Brain and Behavior Research Foundation (Grant Number 28972), BIAL Foundation (Grant Number 099/2020), and individual donors. Dr Marta Bianciardi is supported by the National Institute of Aging (Project Number R01-AG063982), and Michael J. Fox Foundation (MJFF-022672). Dr Terje Sparby is supported by Software AG Stiftung.

Conflict of interest statement: None declared.

Competing interests

The authors declare no competing interests.

Data and materials availability

Data may be requested and subjected to the Institutional Review Board's approval. Code may be made available upon request.

References

Adamaszek M, D'Agata F, Ferrucci R, Habas C, Keulen S, Kirkby KC, Leggio M, Mariën P, Molinari M, Moulton E, et al. Consensus paper: cerebellum and emotion. *Cerebellum*. 2016:16(2):552–576.

Aghabozorgi S, Seyed Shirkhorshidi A, Ying WT. Time-series clustering – a decade review. *Inf Syst*. 2015:53:16–38.

Andrews-Hanna JR, Reidler JS, Sepulcre J, Poulin R, Buckner RL. Functional-anatomic fractionation of the brain's default network. *Neuron*. 2010:65(4):550–562.

Applebaum M. Remembrance: a Husserlian phenomenology of Sufi practice. *J Specul Philos*. 2019:33(1):22–40.

Atasoy S, Roseman L, Kaelen M, Kringelbach ML, Deco G, Carhart-Harris RL. Connectome-harmonic decomposition of human brain activity reveals dynamical repertoire re-organization under LSD. *Sci Rep*. 2017:7(1):17661.

Atasoy S, Vohryzek J, Deco G, Carhart-Harris RL, Kringelbach ML. Common neural signatures of psychedelics: frequency-specific energy changes and repertoire expansion revealed using connectome-harmonic decomposition. *Prog Brain Res*. 2018:242:97–120.

Bates D, Mächler M, Bolker B, Walker S. Fitting linear mixed-effects models using lme4. *J Stat Softw*. 2015:67(1):1–48.

Beauregard M, Paquette V. Neural correlates of a mystical experience in Carmelite nuns. *Neurosci Lett*. 2006:405(3):186–190.

Bianciardi M, Toschi N, Eichner C, Polimeni JR, Setsompop K, Brown EN, Hamalainen MS, Rosen BR, Wald LL. In vivo functional connectome of human brainstem nuclei of the ascending arousal, autonomic, and motor systems by high spatial resolution 7-tesla fMRI. *MAGMA*. 2016:29(3):451–462.

Birn RM, Smith MA, Jones TB, Bandettini PA. The respiration response function: the temporal dynamics of fMRI signal fluctuations related to changes in respiration. *NeuroImage*. 2008:40(2):644–654.

Brahm A. *Mindfulness, bliss, and beyond: a meditator's handbook*. Boston (MA): Wisdom Publications, Inc; 2005.

Brandmeyer T, Delorme A. Reduced mind wandering in experienced meditators and associated EEG correlates. *Exp Brain Res*. 2018:236(9):2519–2528.

Buckner RL, DiNicola LM. The brain's default network: updated anatomy, physiology and evolving insights. *Nat Rev Neurosci*. 2019:20(10):593–608.

Buddhaghoisa B. *Path of purification*. Visuddhimagga: Buddhist Publication Society; 2010.

Buswell RE, Lopez DS, Ahn J, Bass JW, Chu W, Goodman A, Ham HS, Kim S-U, Lee S, PP QA, et al. *The Princeton dictionary of Buddhism*. New Jersey: Princeton University Press; 2014.

Carhart-Harris RL, Leech R, Hellyer PJ, Shanahan M, Feilding A, Tagliazucchi E, Chialvo DR, Nutt D. The entropic brain: a theory of conscious states informed by neuroimaging research with psychedelic drugs. *Front Hum Neurosci*. 2014:8:20.

Cauzzo S, Singh K, Stauder M, Garcia-Gomar MG, Vanello N, Passino C, Staab J, Indovina I, Bianciardi M. Functional connectome of brainstem nuclei involved in autonomic, limbic, pain and sensory processing in living humans from 7 tesla resting state fMRI. *NeuroImage*. 2022:250:1–24, 118925.

Chang C, Cunningham JP, Glover GH. Influence of heart rate on the BOLD signal: the cardiac response function. *NeuroImage*. 2009:44(3):857–869.

Colizoli O, de Gee JW, van der Zwaag W, Donner TH. Functional magnetic resonance imaging responses during perceptual decision-making at 3 and 7T in human cortex, striatum, and brainstem. *Hum Brain Mapp*. 2022:43(4):1265–1279.

Dennison P. The human default consciousness and its disruption: insights from an EEG study of Buddhist Jhana meditation. *Front Hum Neurosci*. 2019:13:178.

Dimidjian S, Segal ZV. Prospects for a clinical science of mindfulness-based intervention. *Am Psychol*. 2015:70(7):593–620.

Ernst CW. The psychophysiology of ecstasy in Sufism and yoga. *N C Med J*. 1998:59:182–184.

Faraguna U, Ferrucci M, Giorgi FS, Fornai F. Editorial: the functional anatomy of the reticular formation. *Front Neuroanat*. 2019:13:55.

Fisher NE. Flavors of ecstasy: states of absorption in Islamic and Jewish contemplative traditions. *Religions*. 2022:13(10):1–26.

Folstein MF, Folstein SE, McHugh PR. "mini-mental state": a practical method for grading the cognitive state of patients for the clinician. *J Psychiatr Res*. 1975:12(3):189–198.

Fox KC, Dixon ML, Nijeboer S, Girn M, Floman JL, Lifshitz M, Ellamil M, Sedlmeier P, Christoff K. Functional neuroanatomy of meditation: a review and meta-analysis of 78 functional neuroimaging investigations. *Neurosci Biobehav Rev*. 2016:65:208–228.

Galante J, Grabovac A, Wright M, Ingram DM, Van Dam NT, Sanguinetti JL, Sparby T, van Lutterveld R, Sacchet MD. A framework for the empirical investigation of mindfulness meditative development. *Mindfulness*. 2023:14(5):1054–1067.

George DT, Ameli R, Koob GF. Periaqueductal Gray sheds light on dark areas of psychopathology. *Trends Neurosci*. 2019:42(5):349–360.

Girn M, Roseman L, Bernhardt B, Smallwood J, Carhart-Harris R, Nathan SR. Serotonergic psychedelic drugs LSD and psilocybin reduce the hierarchical differentiation of unimodal and transmodal cortex. *NeuroImage*. 2022:256:119220.

Glover GH, Li TQ, Ress D. Image-based method for retrospective correction of physiological motion effects in fMRI: RETROICOR. *Magn Reson Med*. 2000:44(1):162–167.

Gunaratana MH. *The Jhanas in Theravada Buddhist meditation*. Sri Lanka: Buddhist Publication Society; 1988.

Hagerty MR, Isaacs J, Brasington L, Shupe L, Fetz EE, Cramer SC. 2013. Case study of ecstatic meditation: fMRI and EEG evidence of self-stimulating a reward system. *Neural Plast* 2013:653572, 1–12.

Kang C, Whittingham K. Mindfulness: a dialogue between Buddhism and clinical psychology. *Mindfulness*. 2010:1(3):161–173.

Keng S-L, Tong EMW, Yan ETL, Ebstein RP, Lai P-S. Effects of mindfulness-based stress reduction on affect dynamics: a randomized controlled trial. *Mindfulness*. 2021:12(6):1490–1501.

Khema A. *Visible here and now: the Buddha's teachings on the rewards of spiritual practice*. Boston, MA: Shambhala Publications; 2001.

King M, Hernandez-Castillo CR, Poldrack RA, Ivry RB, Diedrichsen J. Functional boundaries in the human cerebellum revealed by a multi-domain task battery. *Nat Neurosci*. 2019:22(8):1371–1378.

Kuan T-F. Cognitive operations in Buddhist meditation: interface with western psychology. *Contemporary Buddhism*. 2012:13(1):35–60.

Kuznetsova A, Brockhoff PB, Christensen RHB. lmerTest package: tests in linear mixed effects models. *J Stat Softw*. 2017:82(13):1–26.

Laukkonen RE, Slagter HA. From many to (n)one: meditation and the plasticity of the predictive mind. *Neurosci Biobehav Rev*. 2021:128:199–217.

Laukkonen RE, Sacchet MD, Barendregt H, Devaney KJ, Chowdhury A, Slagter HA. Cessations of consciousness in meditation: advancing a scientific understanding of nirodha samāpatti. *Prog Brain Res*. 2023:280:61–87.

Lieberman MD, Straccia MA, Meyer ML, Du M, Tan KM. Social, self, (situational), and affective processes in medial prefrontal cortex (MPFC): causal, multivariate, and reverse inference evidence. *Neurosci Biobehav Rev*. 2019:99:311–328.

Lindahl JR, Kaplan CT, Winget EM, Britton WB. A phenomenology of meditation-induced light experiences: traditional buddhist and neurobiological perspectives. *Front Psychol*. 2014:4:973.

Lutz A, Thompson E. Neurophenomenology: integrating subjective experience and brain dynamics in the neuroscience of consciousness. *J Conscious Stud*. 2003:10:31–52.

Mahjoory K, Schoffelen JM, Keitel A, Gross J. The frequency gradient of human resting-state brain oscillations follows cortical hierarchies. *elife*. 2020:9:1–18.

Metzinger T. Minimal phenomenal experience. *Philosophy and the Mind Sciences*. 2020:1(I):1–44.

Posit team. *RStudio: integrated development environment for R*. Boston, MA: Posit Software, PBC http://www.posit.co; 2022.

Quadt L, Critchley H, Nagai Y. Cognition, emotion, and the central autonomic network. *Auton Neurosci*. 2022:238:1–12, 102948.

R Core Team. *R: a language and environment for statistical computing*. Vienna, Austria: R Foundation for Statistical Computing; 2022.

Ribas-Fernandes JJF, Shahnazian D, Holroyd CB, Botvinick MM. Subgoal- and goal-related reward prediction errors in medial prefrontal cortex. *J Cogn Neurosci*. 2019:31(1):8–23.

Rolls ET, Cheng W, Feng J. The orbitofrontal cortex: reward, emotion and depression. *Brain Commun*. 2020:2(2):fcaa196.

Sabatinelli D, Bradley MM, Lang PJ, Costa VD, Versace F. Pleasure rather than salience activates human nucleus accumbens and medial prefrontal cortex. *J Neurophysiol*. 2007:98(3):1374–1379.

Sakoe H, Chiba S. Dynamic programming algorithm optimization for spoken word recognition. *IEEE Trans Acoust Speech Signal Process*. 1978:26(1):43–49.

Samuel G. The contemporary mindfulness movement and the question of nonself1. *Transcult Psychiatry*. 2015:52(4):485–500.

Sardá-Espinosa A. Time-series clustering in R using the dtwclust package. *The R journal*. 2019:11(1):22–43.

Sardá-Espinosa A. Dtwclust: time series clustering along with optimizations for the dynamic time warping distance. *Version R package version*. 2023:5(5):11.

Sayadaw P-AT. *Knowing and seeing*. Singapore: Pa-Auk Meditation Centre; 2008.

Schaefer A, Kong R, Gordon EM, Laumann TO, Zuo XN, Holmes AJ, Eickhoff SB, Yeo BTT. Local-global Parcellation of the human cerebral cortex from intrinsic functional connectivity MRI. *Cereb Cortex*. 2018:28(9):3095–3114.

Seo J, Kim DJ, Choi SH, Kim H, Min BK. The thalamocortical inhibitory network controls human conscious perception. *NeuroImage*. 2022:264:1–9, 119748.

Sezer I, Pizzagalli DA, Sacchet MD. Resting-state fMRI functional connectivity and mindfulness in clinical and non-clinical contexts: a review and synthesis. *Neurosci Biobehav Rev*. 2022:135:1–22, 104583.

Sheehan DV, Lecrubier Y, Sheehan KH, Amorim P, Janavs J, Weiller E, Hergueta T, Baker R, Dunbar GC. The mini-international neuropsychiatric interview (M.I.N.I.): the development and validation of a structured diagnostic psychiatric interview for DSM-IV and ICD-10. *The Journal of clinical psychiatry*. 1998:59:22–57.

Sherman SM. Thalamus plays a central role in ongoing cortical functioning. *Nat Neurosci*. 2016:19(4):533–541.

Sherman SM. Functioning of circuits connecting thalamus and cortex. *Compr Physiol*. 2017:7(2):713–739.

Solms M. The hard problem of consciousness and the free energy principle. *Front Psychol*. 2018:9:2714.

Solms M. New project for a scientific psychology: general scheme. *Neuropsychoanalysis*. 2020:22(1–2):5–35.

Sparby T. Phenomenology and contemplative universals- the meditative experience of Dhyana, coalescence, or access concentration. *J Conscious Stud*. 2019:26:130–156.

Sparby T, Sacchet MD. Defining meditation: foundations for an activity-based phenomenological classification system. *Front Psychol*. 2021:12:795077.

Tang YY, Rothbart MK, Posner MI. Neural correlates of establishing, maintaining, and switching brain states. *Trends Cogn Sci*. 2012:16(6):330–337.

Tang YY, Holzel BK, Posner MI. The neuroscience of mindfulness meditation. *Nat Rev Neurosci*. 2015:16(4):213–225.

Tian Y, Margulies DS, Breakspear M, Zalesky A. Topographic organization of the human subcortex unveiled with functional connectivity gradients. *Nat Neurosci*. 2020:23(11):1421–1432.

Tononi G. An information integration theory of consciousness. *BMC Neurosci*. 2004:5(1):42.

Tononi G. Consciousness as integrated information: a provisional manifesto. *Biol Bull*. 2008:215(3):216–242.

Van Dam NT, van Vugt MK, Vago DR, Schmalzl L, Saron CD, Olendzki A, Meissner T, Lazar SW, Kerr CE, Gorchov J, et al. Mind the hype: a critical evaluation and prescriptive agenda for research on mindfulness and meditation. *Perspect Psychol Sci*. 2018:13(1): 36–61.

Venkatraman A, Edlow BL, Immordino-Yang MH. The brainstem in emotion: a review. *Front Neuroanat*. 2017:11:15.

Wassum KM, Izquierdo A. The basolateral amygdala in reward learning and addiction. *Neurosci Biobehav Rev*. 2015:57:271–283.

Wolff M, Vann SD. The cognitive thalamus as a gateway to mental representations. *J Neurosci*. 2019:39(1):3–14.

Wolff M, Morceau S, Folkard R, Martin-Cortecero J, Groh A. A thalamic bridge from sensory perception to cognition. *Neurosci Biobehav Rev*. 2021:120:222–235.

Wright MJ, Sanguinetti JL, Young S, Sacchet MD. Uniting contemplative theory and scientific investigation: toward a comprehensive model of the mind. *Mindfulness*. 2023:14(5):1088–1101.

Yamashiro J. Brain basis of samadhi: the neuroscience of meditative absorption. *New Sch Psychol Bull*. 2015:13:1–10.

Young KS, van der Velden AM, Craske MG, Pallesen KJ, Fjorback L, Roepstorff A, Parsons CE. The impact of mindfulness-based interventions on brain activity: a systematic review of functional magnetic resonance imaging studies. *Neurosci Biobehav Rev*. 2018:84:424–433.

Zang Y, Jiang T, Lu Y, He Y, Tian L. Regional homogeneity approach to fMRI data analysis. *NeuroImage*. 2004:22(1):394–400.